Journal of Bionanoscience
Vol. 12, 1–7, 2018

Transport Properties of Indium Oxide (In_2O_3) Nanofluids Using PVP and Gelatin

KanchanaLatha Chitturi[1], Aparna Yarrama[2,*], Ramchander Merugu[3], and Ravinder Dachepalli[4]

[1] *Department of Physics, Government Degree College Khairthabad, Hyderabad 500004, Telangana, India*
[2] *Department of Physics, JNTUH Kukatpally, Hyderabad 500085, Telangana, India*
[3] *Department of Bio Chemistry, Mahatma Gandhi University, Nalgonda 508254, Telangana, India*
[4] *Department of Physics, Osmania University, Hyderabad 500007, Telangana, India*

Green Bio and Two-step method have been applied for synthesizing Indium oxide nanoparticles and nanofluids respectively with Ethylene Glycol. Indium oxide nanoparticles obtained from Indium (III) Acetylacetonate and Acacia gum were used as precursors. The effect of surfactant PVP (2–5% volume) and Gelatin protein (1% by volume) on Indium oxide nanofluids (1% by volume) was observed. The Indium oxide nanofluids were characterized by UV-Vis Spectroscopy, FTIR, SEM, EDAX, TEM, RAMAN and PL Spectroscopy. The size and morphology from TEM were found to be spherical and 25 nm and 10 nm for 1:2 and 1:5 nanofluids respectively. The effect of PVP and Gelatin protein on thermophysical properties (*Thermal Conductivity*, *Viscosity*, *Density*, *Specific Gravity* and *Ultrasonic Velocity*, *Adiabatic Compressibility* and *Surface Tension*) of Indium oxide nanofluids was observed in the temperature range 30 °C to 60 °C confirming the Newtonian behavior of nanofluid.

Keywords: Green Synthesis, Indium Oxide Nanofluid, Thermophysical Properties, Two-Step Method, TEM, SEM and EDAX, Acacia Gum Mediated, PVP, Gelatin.

RESEARCH ARTICLE

1. INTRODUCTION

The fluid suspensions of nanoparticles called nanofluids by Choi have been found to possess enhanced thermal conductivity and decrement in viscosity to those of base fluids like water, engine oil, etc., which finds potential applications in several fields.

The addition of dispersants and proteins to nanofluids will increase surface area and surface activity and retards the growth and agglomeration of nanoparticles by *Steric Effect*. It is an easy and economic method to enhance the stability of nanofluids and also for heat transfer applications. For oxide nanoparticles, the *Two-step method* is a stable method and its stability is determined by *UV-Vis Spectrophotometer*. With nanoparticle loading of 1% to volume of base fluid, the thermal conductivity is enhanced and the viscosity decremented. The decremented viscosity reduces pressure drop in heat transfer and density determines the behavior of fluids. Proteins *in vivo* are very complex biological systems. Inside the cell the nanoprotein complexes may be processed by different cellular pathways. This processing inside the cellular environment may make the protein nano interaction constantly changing. The protein can absorb or desorb the nanoparticles at different phases within the cell.[1,2] Generally protein nanoparticle interactions are used as a model system for studying possible biological interactions inside the body.[3] Nanoparticle surface may get pre-coated with specific proteins inside a cellular environment. Bovine serum albumin protein binding to Gold nanoparticles was found to adsorb strongly to a pegylated/neutral surface.[4,5] Bio functionalized silver nanoparticles with reduced aggregation were reported to be more suitable for bio-sensing applications.[6] The synthesis of Indium Oxide nanofluid is similar to our earlier work reported in our paper.[7]

2. EXPERIMENTAL DETAILS

2.1. Fabrication of In_2O_3 Nanoparticles and In_2O_3 Nanofluid

8 g of *Indium (III) Acetylacetonate* (*Sigma-Aldrich*) is mixed with 0.8 g of *Acacia gum* (bought from local *Unani Medical Shop* at Hyderabad) and were finely powdered using mortar and pistle. The mixture is characterized by TGDTA. The calcination temperature is found to be 400 °C. The yellowish Indium Oxide nanoparticles were obtained after calcining for 2 hours in air. The obtained

*Author to whom correspondence should be addressed.

Indium oxide nanoparticles of (volume % = 1) is dispersed in Ethylene glycol base fluid and sonicated for about 30 minutes at room temperature and then added the surfactant PVP (2 to 5%) and Gelatin protein (volume % = 1) and again sonicated for about 30 minutes at room temperature and then added NaOH of *pH* adjustment (7–8) to obtain Indium oxide nanofluid, which is a *Two-step method* suitable for oxide nano particles.

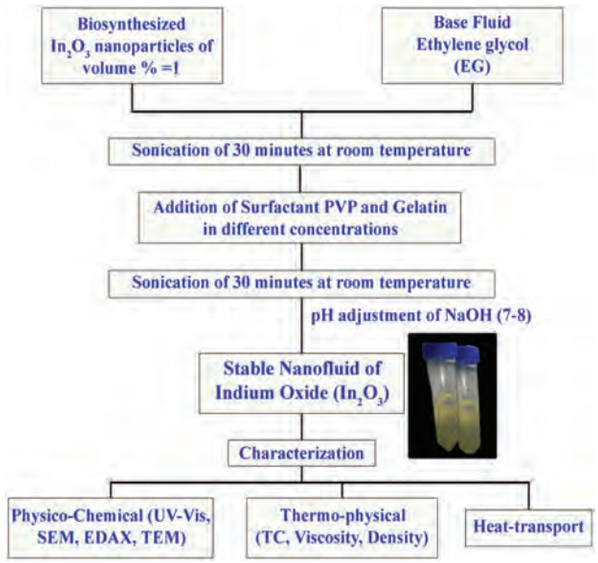

2.2. Characterization of Nanofluids

UV-Vis absorption spectrum (*SHIMDAZU*) has been recorded on *NanoDrop 1000 Spectrophotometer* 1-mm column in the wave length range 200 to 600 nm at room temperature. SEM and EDAX of Indium Oxide nanofluids on glass substrate were taken using *HITACHI*. TEM images have been taken by placing the nanofluid directly on copper grid and allowing the sample to evaporate naturally. FTIR, RAMAN and PL spectrum was taken. In the temperature range of 30–60 °C, the density and specific gravity of nanofluids were measured using *ANTON PAAR Density Meter* and the viscosity by *CANNON-FENSKE Kinematic Viscometer*. Electrical conductivity measurements at room temperature for different concentrations were obtained with the aid of *Microprocessor based Conductivity Meter*. For measuring the thermal conductivity of nanofluids Steady state parallel method (*Hilton Thermal Conductivity of liquids and gases Unit H471*) was used which is expressed as

$$K = \frac{Q_c \Delta r}{A \Delta t}$$

where, Q_c—Heat transfer by conduction through the base fluid; Δr—Radial Clearance, A—Area of conduction path, and Δt—Temperature difference. So that the heat transfer co-efficient is in linear behavior with respect to voltage. *Nanofluid Interferometer NF-12X* is used to measure the *ultrasonic velocity*, *adiabatic compressibility* and *surface tension*.

Table I. Parameters for synthesis of In_2O_3 nanofluids.

In_2O_3:PVP:Gelatin weight ratio	Description
(Sample-1)1:2:1	0.2 g of In_2O_3 with 0.4 g of PVP and 0.2 g of Gelatin in 200 ml EG
(Sample-2)1:5:1	0.2 g of In_2O_3 with 1 g of PVP and 0.2 g of Gelatin in 200 ml EG

3. RESULTS AND DISCUSSION

Nanoparticles entering the body are shaped by sequential exposure to different protein rich environments. Kinetics of protein adsorption on the NP surface differs for different proteins. Monopoli et al., reported that the protein absorption varied with increasing protein plasma concentration. This may result in the formation of different nanocomposites inside the cell. Pre-coating of pulmonary surfactant proteins was found to influence the subsequent adsorption of plasma proteins on carbon nanotubes.[8] Human Serum Albumin (HSA) and transfer in adsorbed in a monolayer fashion on Iron-Platinum (FePt) nanoparticle surface and Aluminium Oxide surface.[9, 10]

3.1. UV-Vis Analysis

The room temperature UV-Vis absorption spectrum of the In_2O_3 nanofluids is recorded in the wave length range of 200–800 nm. Figure 1 represents the spectrum which has a peak at 277 nm (4.4 eV for sample 1) and 318 nm (3.9 eV for sample 2). The absorption peak for 12 nm In_2O_3 nanoparticle has been reported at 270 nm (3.6 eV). The obtained nanofluids has excellent stability which gives the same absorbance peak value for every 4 hours in 24 hours

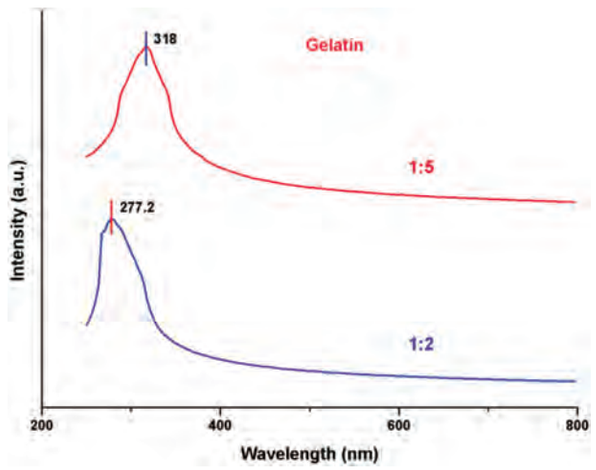

Fig. 1. UV-vis absorption spectrum of sample-1 and sample-2 of indium oxide nanofluids.

RESEARCH ARTICLE

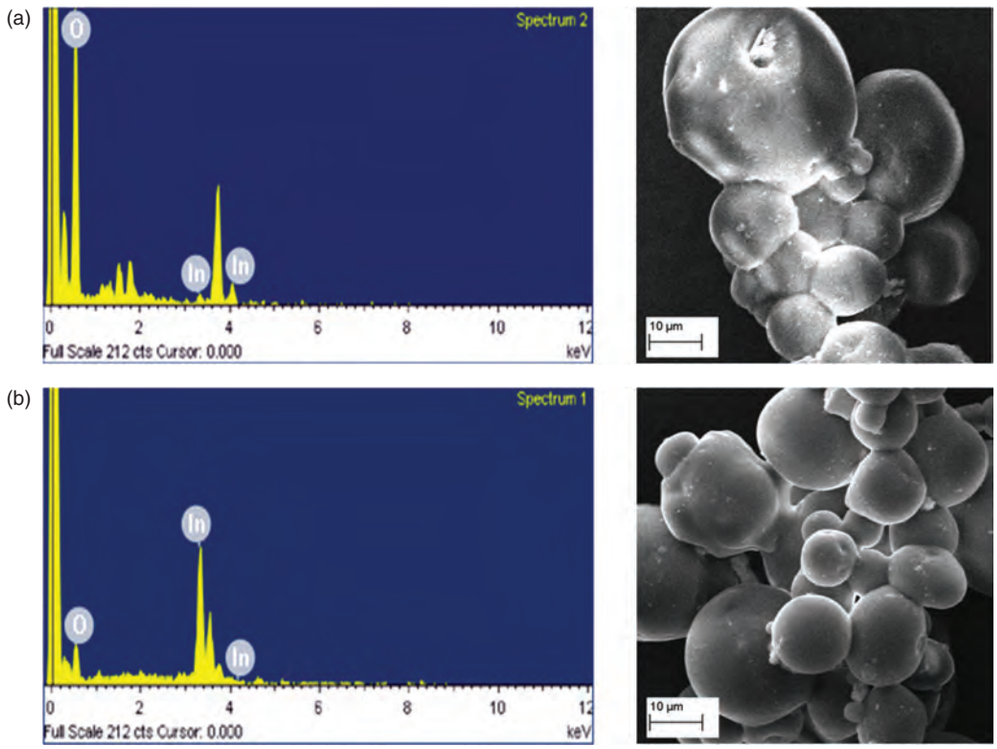

Fig. 2. EDAX and SEM of sample-1 and sample-2 of indium oxide nanofluids.

and are stable for 15 days. The variation in absorption peak of (sample 1 and sample 2) is due to the variation of concentration of PVP. Thus at a nanoscale the bandgap decreases for the In_2O_3 nanofluid (sample 2) with excellent stability due to the protection role of PVP and Gelatin protein.[11]

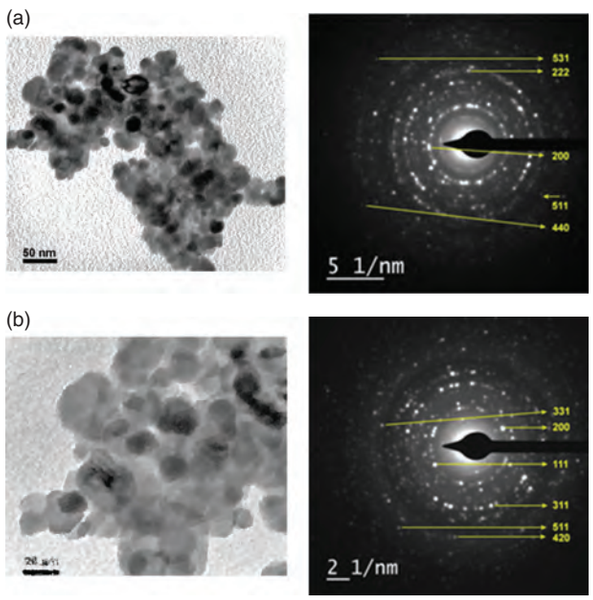

Fig. 3. TEM and SAED patterns of sample-1 and sample-2 of indium oxide nanofluids.

3.2. EDAX and SEM Analysis

In Figure 2, the EDAX spectrum of the In_2O_3 nanofluids reveals that the (sample 1 and sample 2) containing '*In*' and '*O*' as main constituent components indicate no contamination is present due to PVP and Gelatin proteins and their atomic and weight ratios confirm the literature values. The SEM images of In_2O_3 nanofluids of (samples 1 and 2) show the random distribution of nanoparticles having *spherical* shape of large surface area with porous nature.

3.3. TEM and SAED Analysis

Figure 3 shows the TEM and SAED images of sample 1 and sample 2 of In_2O_3 nanofluids. The TEM images reveal that the nanoparticles are *spherical* in shape of size 25 nm for sample 1 and 10 nm for sample 2. The SAED patterns

Table II. Interplanar spacings of In_2O_3 nanofluid (with Gelatin protein) from SAED patterns (in Fig. 3).

Ring no.	In_2O_3 nanofluid		Standard JCPDS: 06-0416	
	Sample 1 d_{hkl} (Å)	Sample 2 d_{hkl} (Å)	d_{hkl} (Å)	hkl
R1	1.0309	1.0077	1.0414	511
R2	1.587	1.556	1.5622	222
R3	2.797	2.7609	2.7056	200
R4	1.935	2.205	1.9134	220
R5	0.969	–	0.9566	440
R6	1.356	1.359	1.353	400
R7	–	1.6926	1.6318	311

RESEARCH ARTICLE

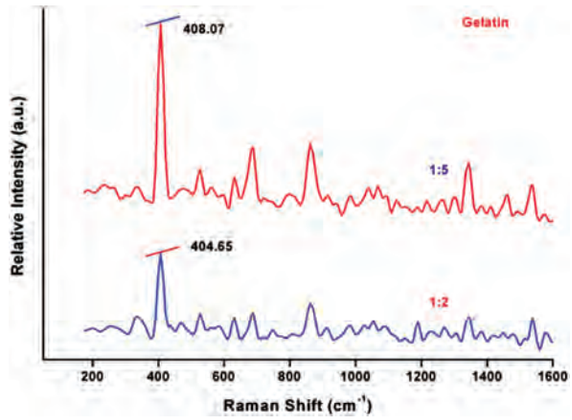

Fig. 4. Raman spectra of sample-1 and sample-2 of indium oxide nanofluids.

of the two samples reveal polycrystalline structure of In_2O_3 nanoparticles. The interplanar spacings obtained for different *hkl* values are consistent with *Standard Data* (*JCPDS no.06-0416*) of the two samples as shown in Table II.

3.4. Raman Spectra Analysis

Figure 4 shows the Raman Spectra of sample 1 and sample 2 with expected vibrational modes at 407 cm^{-1}, 870 cm^{-1}, 1300 cm^{-1}. These peaks of the samples 1 and 2 confirm the pure In_2O_3 vibrational modes.

Table III. FTIR data of In_2O_3 samples capped with sample-1 and sample-2.

	C–H vibration	Adsorption of C═O vibration	C═O vibration from acetyl-acetonate specia
Sample-1	2943 cm^{-1}	1651 cm^{-1}	1407 cm^{-1}
Sample-2	2940 cm^{-1}	1655 cm^{-1}	1404 cm^{-1}

3.5. FTIR Analysis

Figure 5 shows the IR Spectra of sample 1 and sample 2 indicating that the bands around 2943 cm^{-1} (sample 1) and 2940 cm^{-1} (sample 2) can be ascribed to the C–H vibrations of the organics while the absorptions around 1407 cm^{-1} (sample 1) and 1404 cm^{-1} (sample 2) are due to In–O vibrations.[12] This indicates the presence of PVP and Gelatin on the surface species of the In_2O_3 nanocrystals as shown in Table III.

3.6. PL Analysis

In Figure 6, PL Spectra of sample 1 and sample 2 show a weak UV-band at 340 nm and 348 nm respectively. It is well known that a bulk In_2O_3 cannot emit light at room temperature. PL emissions of In_2O_3 nanofluid are due to the effect of oxygen vacancies.

3.7. Thermo Physical Analysis

Figure 7 represents the voltage versus thermal conductivity. The ratio of K_{eff}/K_b is a non-linear behavior in sample 1 and a sharp increase with increase of voltage for sample 2. It can be explained, based on Brownian motion that nanoparticles are freed from PVP binding due to increase in temperature diffusing through the polymer matrix.[13] Thermal vibrations cause polymer to lose its

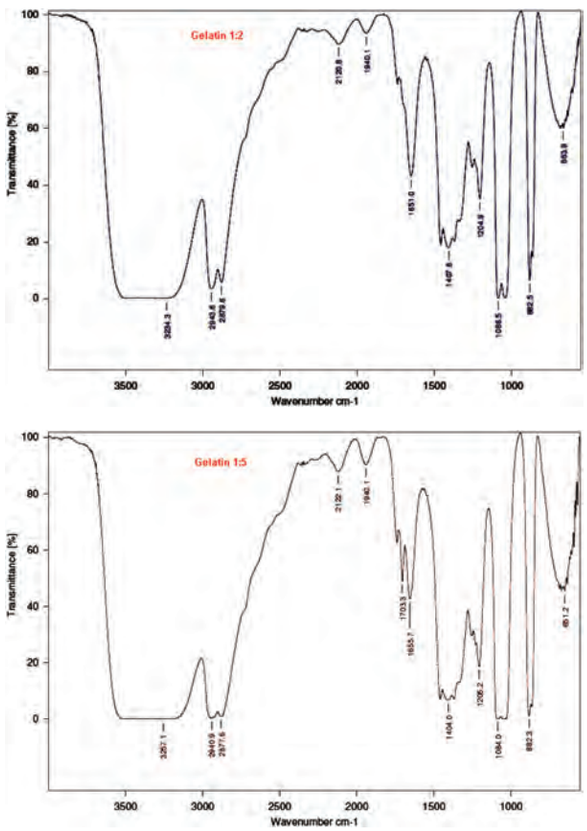

Fig. 5. FTIR spectra of sample-1 and sample-2 of indium oxide nanofluids.

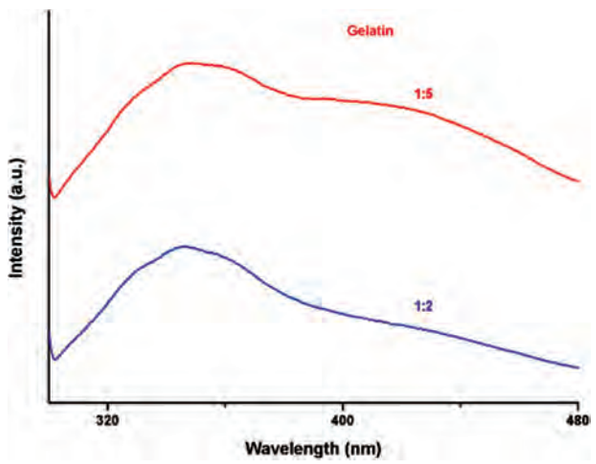

Fig. 6. PL spectra of In_2O_3 samples capped with sample-1 and sample-2.

RESEARCH ARTICLE

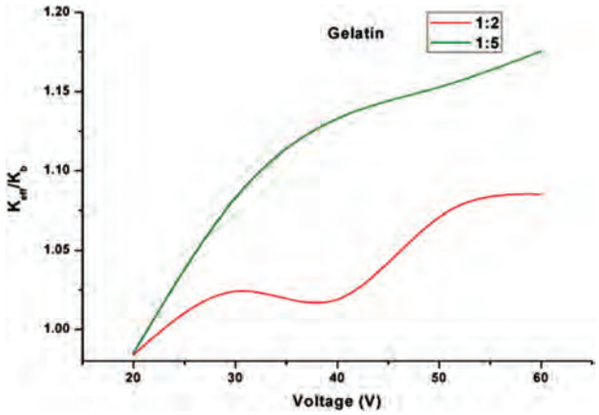

Fig. 7. Voltage versus thermal conductivity enhancement ratio (K_{eff}/K_b) for indium oxide nanofluids (sample-1 and sample-2).

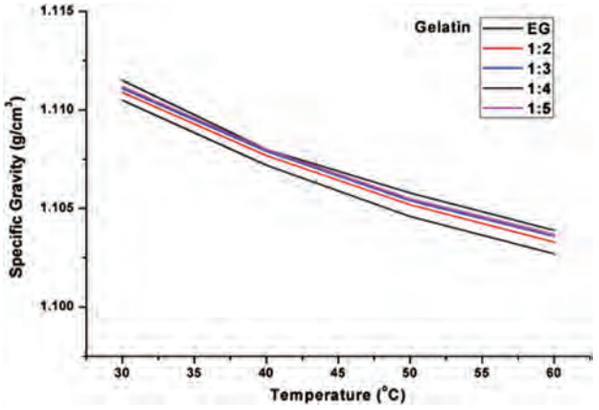

Fig. 9. Temperature versus specific gravity of indium oxide nanofluids (sample-1 and sample-2).

structure allowing greater surface area to nanoparticles to take part in heat transfer. The enhancement of TC with voltage from 40 V of sample 2 may be due to polymer and Gelatin protein ligand binding which are considered as important mechanism for enhancing TC of nanofluid[14–20] and the percentage of enhancement of sample 2 is found to be 30% compared to that of Ethylene Glycol base fluid.

Figures 8 and 9 represents the density and specific gravity versus temperatures ranging from 30 °C to 60 °C. Density and specific gravity increases with increase of concentration of PVP than that of basefluid. Further it is observed that at higher temperature (50–60 °C) density of sample 2 decreases with that of base fluid Ethylene glycol indicating that the behaviour of protein interaction with nanofluids is good for heat transfer application.

Figure 10 represents that viscosity of nanofluid decreases with increase of temperature than that of base fluid confirming that protein interaction nanofluid reduces pressure drop in heat transfer as compared with that of the base fluid.

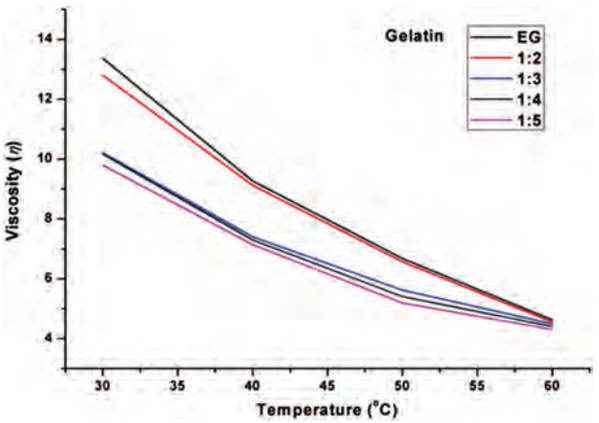

Fig. 10. Temperature versus viscosity of indium oxide nanofluids (sample-1 and sample-2).

Figure 11 shows the plot of ultrasonic velocity of (sample 1, sample 2) and basefluid as a function of temperature. A non-linear relation between velocity and temperature and linear at a temperature range of 50 °C to 60 °C.

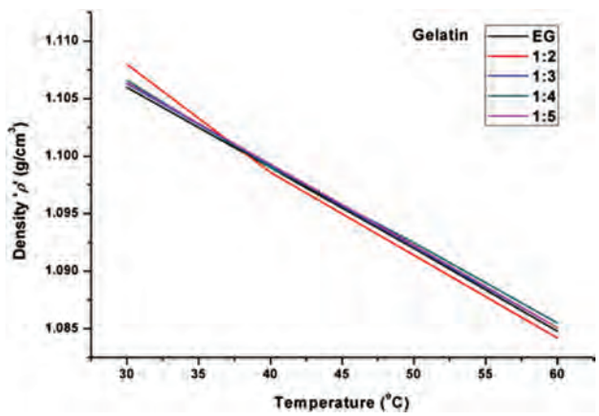

Fig. 8. Temperature versus density of indium oxide nanofluids (sample-1 and sample-2).

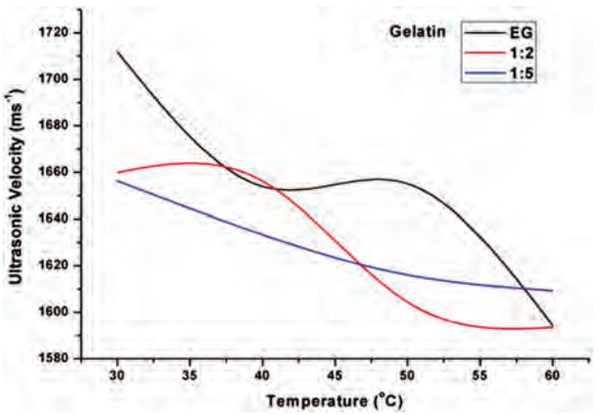

Fig. 11. Temperature versus ultrasonic velocity of indium oxide nanofluids (sample-1 and sample-2).

RESEARCH ARTICLE

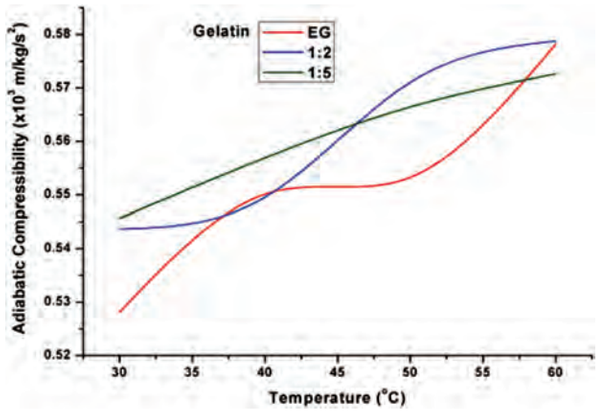

Fig. 12. Temperature versus adiabatic compressibility of indium oxide nanofluids (sample-1 and sample-2).

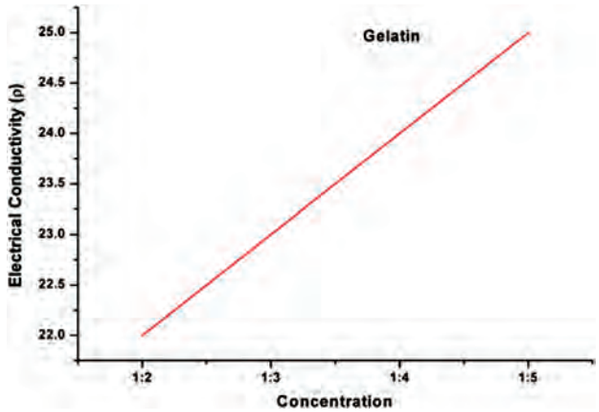

Fig. 14. Concentration versus electrical conductivity of In_2O_3 nanofluids (sample-1 and sample-2).

As the concentration of PVP is increased the ultrasonic velocity gets enhanced, decreasing adiabatic compressibility (Fig. 12). The decrease is attributed to the fact that strong cohesive interaction forces act among the molecules and atoms after the dispersion of In_2O_3 nanoparticles in PVP and polymer matrix.[21–25] It is observed that as temperature increases above 50 °C naoparticles diffuse through the polymer matrix and ultrasonic vibrations cause polymer to lose its structure allowing greater surface area to nanoparticles to take part in heat transfer.

In Figure 13, the surface tension (of sample 2) gets enhanced with the increase of temperature than in (sample 1) and base fluid. In Figure 14, the electrical conductivity of In_2O_3 nanofluids shows linear behaviour with increase of concentration of PVP than that of ethylene glycol. Interaction of nanoparticles results in the formation of a nanoparticle-protein corona. The protein corona influences the processing of the nanoprotein complexes which plays an important role in the immunological response towards a protein nanocomposite.[26]

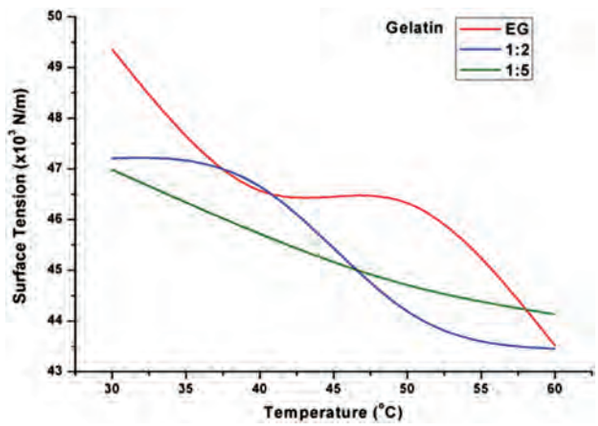

Fig. 13. Temperature versus surface tension of indium oxide nanofluids (sample-1 and sample-2).

4. CONCLUSION

We have successfully synthesised the Indium Oxide nanoparticles and nanofluid of (sample 1 and sample 2) by green and two step method respectively. The dispersed nanoparticle of In_2O_3, Gelatin protein and different concentration of PVP and their thermo physical properties were observed with thermal conductivity enhancement and decrement in viscosity with increase in concentration of PVP. This can be applied in industrial cooling applications.

References and Notes

1. E. Casals, T. Pfaller, A. Duschl, G. J. Oostingh, and V. Puntes, *ACS Nano* 4, 3623 (**2010**).
2. S. Ozerinc, S. Kakac, and A. G. Yazlcloglu, *Micro fluidics and Nanofluidic* 8, 145 (**2010**).
3. R. Žūkienė and V. Snitka, *Biointerfaces* 135, 316 (**2015**).
4. S. P. Boulos, T. A. Davis, J. A. Yang, S. E. Lohse, A. M. Alkilany, L. A. Holland, and C. J. Murphy, *Langmuir* 29, 14984 (**2013**).
5. M. P. Monopoli, D. Walczyk, A. Campbell, G. Elia, I. Lynch, F. BaldelliBombelli, and K. A. Dawson, *J. Am. Chem.* 133, 2525 (**2011**).
6. M. Ashok and N. Chandrasekaran, *Colloids and Surfaces B: Biointerfaces* 76, 32 (**2010**).
7. Ch. KanchanaLatha, Y. Aparna, M. Ramchander, and D. Ravinder, *International Journal of Engineering Research and Applications* 6, 94 (**2016**).
8. M. Gasser, B. Rothen-Rutishauser, H. F. Krug, P. Gehr, M. Nelle, and P. B. Yan, *J. Nanobiotechnology* 8, 1477 (**2010**).
9. J. Xiue, W. Stefan, M. Hafner, C. Röcker, F. Zhang, J. Wolfgang, and G. UlrichNienhaus, *J. Royal Soc. Interface* 7, 5 (**2009**).
10. R. Kurosch, P. Lorenz, R. Mandana, V. Janos, T. Marcus, and J. Ludwig, *Langmuir* 20, 10055 (**2004**).
11. Z. Shervani, Y. Ikushima, M. Sato, H. Kawanami, Y. Hakuta, T. Yokoyama, T. Nagase, and K. Aramaki, *Colloid PolymSci.* 7, 1784 (**2007**).
12. W. H. Ho and S. K. Yen, *Thin Solid Films* 498, 80 (**2006**).
13. K. Das, N. Putra, P. Thiesen, and W. Roetzl, *J. Heat Transfer* 125, 567 (**2003**).
14. H. C. Chon, K. Kihm, S. P. Lee, and S. U. S. Choi, *ApplPhysLett.* 87, 153107 (**2005**).
15. J. C. Maxwell, *Clarendon* (**1891**).

RESEARCH ARTICLE

16. X. Wang and A. Mujumdar, *Int. J. Thermal Sci.* 46, 1 **(2007)**.
17. L. Kathy and C. Kessler, *J. Mater. Sci.* 41, 5613 **(2007)**.
18. W. Yu, H. Xie, Chen, and L. Li, *ThermochimActa* 491, 92 **(2009)**.
19. D. Li, Xie, and W. Fang, *Nanoscale Res. Lett.* 373, 1 **(2011)**.
20. H. Chang, C. Jwo, C. Lo, T. Tsung, M. Kao, and H. Lin, *Rev. Adv. Mater. Sci.* 10, 128 **(2006)**.
21. H. Chang and M. H. Tsai, *Rev. Adv. Mater. Sci.* 18, 734 **(2008)**.
22. S. Temkin, *J. Acoust. Soc. Am.* 103, 838 **(1998)**.
23. T. E. Gomez Alvarez, et al., *Ultrasonics* 39, 715 **(2002)**.
24. D. K. Singh, D. K. Pandey, and R. R. Yadav, *Ultrasonics* 49, 634 **(2009)**.
25. A. Jozefczak and A. Skumiel *J. Phys. Condens. Matter.* 18, 1869 **(2006)**.
26. R. Saptarshi, A. Duschl, and A. L. Lopata, *Journal of Nanobiotechnology* 11, 26 **(2013)**.

Received: xx Xxxx xxxx. Accepted: xx Xxxx xxxx.